Contemporary Mathematics
https://ojs.wiserpub.com/index.php/CM/

Research Article

Analytical and Numerical Treatment of an Integro Partial Differential Equation in Position and Time with an Anomalous Position Kernel

Azhar Rashad Jan

Mathematics Department, Faculty of Sciences, Umm Al-Qura University, Makkah, Saudi Arabia
E-mail: arjaan@uqu.edu.sa

Received: 13 May 2025; **Revised:** 16 June 2025; **Accepted:** 14 July 2025

Abstract: This work presents a second-order Integro-Partial Differential Equation (Io-PDE) with respect to time and space, incorporating a generalized anomalous spatial kernel $k(|x-y|)$, $-1 \leq x, y \leq 1$. From this general kernel, one can derive many special kernels, such as the logarithmic and Carleman types, the Cauchy kernel, and the strongly anomalous kernel. Other special cases can also be derived from the proposed generalized kernel. A delayed-phase formulation is also extracted as a specific instance. By imposing initial conditions, the Io-PDE is reformulated as a Mixed Integral Equation (MIE) defined in both space and time domains. We establish the uniqueness and existence of a solution and demonstrate the convergence properties. A separation of variables approach is then applied, leading to a System of Fredholm Integral Equations (SFIEs) characterized by singular spatial kernels and time-dependent coefficients. The Toeplitz Matrix Method (TMM), known for its robustness in handling anomalous equations, is utilized to numerically solve these SFIEs. This method simplifies complex anomalous integrals into standard numerical forms. Numerical experiments are conducted using logarithmic and Carleman kernels, and associated error metrics are evaluated.

***Keywords*:** Integro-Partial Differential Equation (Io-PDE), Mixed Integral Equation (MIE), the anomalous kernel, technique of separation, Toeplitz Matrix Method (TMM)

MSC: 45K05, 65R20

1. Introduction

Mathematical modeling of complex physical and engineering systems often leads to equations involving integral and differential terms. These models are instrumental in describing processes with memory effects or nonlocal behavior. One such class of models is the Integro-Partial Differential Equation (Io-PDE), which has gained prominence due to its ability to capture time and space dependencies with anomalous behavior.

Numerous researchers have contributed to the study of Mixed Integral Equations (MIEs), which combine properties of both Volterra and Fredholm equations. Abdou [1] explored Fredholm-Volterra integral equations of the first kind in the context of contact problems, highlighting their mathematical structure and importance. In a subsequent work, Abdou [2] addressed both linear and nonlinear integral equations, providing a comprehensive analysis of their properties and methods of solution.

DOI: https://doi.org/10.37256/cm.6420257224

Alahmadi et al. [3] applied the Adomian Decomposition Method and the Homotopy Analysis Method to numerically solve a nonlinear Fredholm integral equation in two dimensions, demonstrating the applicability of semi-analytical techniques to such problems. Matoog et al. [4] used the Genocchi polynomial approach to approximate solutions for nonlinear fractional integral equations, showing effective convergence properties. Raad and Abdou [5] developed an algorithm for solving integro-fractional differential equations with generalized symmetric singular kernels, employing the Toeplitz Matrix Method (TMM) to handle these complex structures.

Rostami and Maleknejad [6] used hybrid Bernstein polynomials and block-pulse functions to numerically solve fractional Volterra-Fredholm integral partial differential equations with weak singularities in space and time. In a related work, Abdou et al. [7] analyzed the behavior of maximum and minimum errors in Fredholm-Volterra integral equations within two-dimensional spaces, offering insights into the nature of error propagation.

Basseem and Alalyani [8] employed orthogonal polynomial techniques to study nonlinear mixed functional-Volterra integral equations with continuous kernels. Matoog [9, 10] provided evidence for the existence of at least one solution to singular Volterra-Hammerstein integral equations and proposed modified Taylor methods for their numerical solution. Micula [11] advanced iterative techniques for Volterra functional integral equations of the second kind, focusing on convergence and stability.

Mirzaee et al. [12] applied the Fibonacci collocation method to Volterra-Fredholm integral equations, illustrating the strength of non-classical bases in approximating integral equations. Nasr and Abdel-Aty [13] examined the regularity and consistency of MIEs with continuous kernels, while Matoog [14] investigated potential kernels in nuclear integral equations. Basseem [15] addressed degenerate kernel methods for three-dimensional integral equations, and Abdou et al. [16] studied quadratic phase-lag integral equations from both theoretical and computational perspectives.

In the domain of hybrid numerical methods, Rostami and Maleknejad [17, 18] discussed solutions for two-dimensional nonlinear mixed partial integro-differential equations using modified block-pulse functions and Bernoulli polynomials. Their techniques accounted for both initial conditions and operational matrices. Xie [19] introduced the use of modified fractional Legendre wavelets to compute solutions to fractional PDEs with variable coefficients. Xie et al. [20] further implemented Haar wavelets to solve coupled systems of fractional-order integral-differential equations, while in a separate study, Xie et al. [21] employed two-dimensional Chebyshev wavelets to tackle time-space fractional Fokker-Planck equations. Jan [22] previously proposed a model for solving mixed fractional integro-differential equations, which laid the groundwork for extending these ideas to more generalized anomalous kernels. The current study builds upon these earlier contributions by presenting a comprehensive analytical and numerical investigation of a generalized Io-PDE model. The paper introduces a general form of an anomalous spatial kernel and demonstrates how classical kernels, such as logarithmic and Carleman types, emerge as special cases. By transforming the Io-PDE into a Volterra-Fredholm type MIE using initial conditions, the work establishes the existence, uniqueness, and convergence of the solution.

Sayed et al. [23] solved the hyperbolic telegraph equation in both one and two dimensions, after applying the Galerkin method. Ezz-Eldien and Alalyani [24] used the Legendre spectral collocation method to solve the Volterra-Fredholm integral equation in two dimensions. Yassin et al. [25] used numerical solutions for solving nonlinear ordinary and fractional Newell-Whitehead-Segel equations. Abd-Elhameed et al. [26] used the orthogonal polynomial method of seventh-kind Chebyshev polynomials for solving fractional delay differential equations.

The Toeplitz Matrix Method (TMM), as demonstrated by Abdou et al. [27], is adopted for its computational efficiency and suitability for handling anomalous kernels. This method not only reduces complex integrals to numerically tractable forms but also exhibits strong convergence behavior. Through the use of numerical examples involving various kernels, the proposed framework is validated, offering promising avenues for future exploration in nonlinear cases and high-dimensional settings.

In the remainder part of this work, especially in Section 2, we establish many special cases from the principal integro partial differential equation and the kernel of the equation. For example, the logarithmic kernel, the Carleman function, the Hilbert kernel, the Cauchy kernel, and the strong singular kernel are considered special cases of the general kernel. Moreover, after integrating and using the initial conditions, we obtain a MIE of Volterra-Fredholm type.

In Section 3, using Banach's fixed point theorem, we prove the existence of a unique solution. In Section 4, the convergence of the solution is discussed. In Section 5, we represent the function of the error as a MIE of Volterra-Fredholm type, and then the stability of the error is proved.

In Section 6, a technique of separation is used to transform the MIE to an FIE of the second kind in position, in addition, the coefficients of the FIE are variable in time. In Section 7, the TMM, as a numerical method is used to transform the FIE to a linear algebraic system. In Section 8, Certain values of the constants were assumed as well as the analytical solution, and the compact matrix method was applied to the logarithmic kernel as well as the Carleman kernel in the form of three successive applications in which the time varies. Indeed, it was shown from the tables that the longer the cumulative time, the greater the cumulative error. These results and expressions are presented in Section 9. In Section 10, the importance of the results obtained and the importance of work in general are written.

2. Principal integral equation and time phenomenon

In this section, the equation shown will be linked to the time delay equation, with some special cases being deduced.

$$\lambda_1 \frac{\partial^2}{\partial t^2}\Phi(x;t)+\lambda_2 \frac{\partial}{\partial t}\Phi(x;t)+\lambda_3\Phi(x;t)-g(t)\int_{-1}^{1}k(|x-y|)\Phi(y;t)dy=f(x;t);$$
$$\left\{\frac{\partial}{\partial t}\Phi(x;0)=\Psi_1(x),\quad \Phi(x,0)=\Psi_2(x)\right\}. \tag{1}$$

Special cases from the integrodifferential equation:

1. Let $\lambda_1=0$, $F(t)=\delta-$ cons $\tan t$, we have the initial value problem

$$\lambda_2 \frac{\partial}{\partial t}\Phi(x;t)+\lambda_3\Phi(x;t)-\delta\int_{-1}^{1}k(|x-y|)\Phi(y;t)dy=f(x;t);\quad \{\Phi(x,0)=\Psi_2(x)\} \tag{2}$$

The previous initial value problem is solved by Jan [22].

2. Equation (1) is equivalent to the phase-lag integral equation

$$\mu\Phi(x;t+q)-g(t)\int_{-1}^{1}k(|x-y|)\Phi(y;t)dy=f(x;t);\quad \left\{\frac{\partial}{\partial t}\Phi(x;0)=\Psi_1(x),\quad \Phi(x,0)=\Psi_2(x)\right\} \tag{3}$$

Phase lag problems play a prominent role in explaining many physical phenomena in all different sciences. Phase lag comes and explains its temporal effect on the development of the physical properties of matter. This temporal lag is always related to the differential derivatives of the equations, which means the order of dissociation of the ionic bond between the molecules of the substance. Hence the importance of studying the initial conditions issues.

3. Many special cases can be derived from the general form of the kernel $k(|x-y|)$.

In this section, the researcher deduces many forms of special anomalous nuclei from the imposed general nucleus.

(3.1) Logarithmic kernel $k(|x-y|)=\ln|x-y|$.

(3.2) Carleman kernel $k(|x-y|)=|x-y|^{-\nu}$, $0\le\nu<1$.

(3.3) Hilbert kernel $k(|x-y|)=\cot\frac{|x-y|}{2}$.

(3.4) Cauchy kernel $k(|x-y|)=\frac{1}{|x-y|}$.

(3.5) Strong singular kernel $k(|x-y|)=\frac{1}{(x-y)^2}$.

Now, integrating Eq. (1) and using the initial conditions, for the first integral, we get

$$\lambda_1 \frac{\partial \Phi(x;t)}{\partial t} + \lambda_2 \Phi(x;t) + \lambda_3 \int_0^t \Phi(x;\tau)d\tau - \int_0^t \int_{-1}^1 g(\tau)k(|x-y|)\Phi(y;\tau)dyd\tau$$

$$= \int_0^t f(x;\tau)d\tau + \lambda_1 \psi(x) + \lambda_2 \psi(x) \tag{4}$$

For the second integral, we have

$$\Phi(x;t) + \frac{1}{\lambda_1}\int_0^t [\lambda_2 + \lambda_3(t-\tau)]\Phi(x;\tau)d\tau - \frac{1}{\lambda_1}\int_0^t \int_{-1}^1 (t-\tau)g(\tau)k(|x-y|)\Phi(y;\tau)dyd\tau = \frac{1}{\lambda_1}H(x,t)$$

$$H(x,t) = \int_0^t (t-\tau)f(x;\tau)d\tau + \lambda_1 t\psi_1(x) + \lambda_2 t\psi_2(x) + \lambda_1\psi_1(x) \tag{5}$$

The formula (5) is called MIE in position and time. The second term of (3) takes the Volterra integral (VI) with Abel kernel and the third term takes the Volterra-Fredholm integral (V-FI) with two singular kernels. Also, the free term contains after integrating Abel's kernel.

3. Existence and uniqueness solution of the mixed integral equation

In this section, the researcher proves the existence and uniqueness of the solution to the mentioned mixed equation. For this aim, write (5) in the integral operator form

$$\overline{W}\Phi(x;t) = \frac{1}{\lambda_1}H(x;t) + \frac{1}{\lambda_1}W_1\Phi(x;t) + \frac{1}{\lambda_1}W_2\Phi(x;t)$$

$$W_1\Phi(x;t) = -\int_0^t [\lambda_2 + \lambda_3(t-\tau)]\Phi(x;\tau)d\tau \tag{6}$$

$$W_2\Phi(x;t) = \int_0^t \int_{-1}^1 (t-\tau)g(\tau)k(|x-y|)\Phi(y;\tau)dyd\tau$$

Then, assume the following conditions:
(i) The kernel of position satisfies the discontinuous condition

$$\left\{\int_{-1}^1 \int_{-1}^1 |k(|x-y|)|^2 dxdy\right\}^{\frac{1}{2}} = C. \qquad \text{(C-constant)} \tag{7}$$

(ii) The given function $H(x,t)$ with its partial derivatives with respect to position x and time t are continuous in the space $L_2(-1,1)\times C[0,T]$, and its norm is defined as

$$\|H(x;t)\|_{L_2(-1,1)\times C[0,T]} = \max_{0\le t\le T}\left|\int_0^t \left\{\int_{-1}^1 |H(x;\tau)|^2 dx\right\}^{\frac{1}{2}} d\tau\right| = G$$

$$G = \frac{T^2}{2} f + \lambda_1 \psi_1 T + \lambda_2 \psi_2 T + \lambda_1 \psi_1, \quad (f,\ \psi_1,\ \psi_2 - \text{ cons tan} ts) \tag{8}$$

where

$$f(x;t) \in L_2(-1,1)\times C[0,T], \quad \to \quad \|f(x;t)\|_{L_{2(-1,1\times C[0,T]}} = \max_{0\le t\le T}\left|\int_0^t \left\{\int_{-1}^1 |f(x;\tau)|^2 dx\right\}^{\frac{1}{2}} d\tau\right| = f$$

$$|\psi_1(x)| \le \psi_1,\ |\psi_2(x)| \le \psi_2,\ T = \max t \tag{9}$$

(iii) The norm of the unknown function in $L_2(-1,1)\times C[0,T]$-space is

$$\|\Phi(x;t)\|_{L_2(-1,1)\times C[0,T]} = \max_{0\le t\le T}\left|\int_0^t \left\{\int_{-1}^1 |\Phi(x;\tau)|^2 dx\right\}^{\frac{1}{2}} d\tau\right| = r. \tag{10}$$

To discuss the existence and uniqueness of the solution we must prove the following:

Lemma 1 Under the assumptions (i)-(iii), the integral operator $\overline{W}$ maps the space $L_2(-1,1)\times C[0,T]$ into itself.

Proof. Write the integral operator $\overline{W}$, with the aid of Cauchy-Schwartz inequality, in the form

$$\|\overline{W}\Phi(x;t)\| \le \left|\frac{1}{\lambda_1}\right| \|H(x;t)\| + \left|\frac{1}{\lambda_1}\right| \|W_1\Phi(x;t)\| + \left|\frac{1}{\lambda_2}\right| \|W_2\Phi(x;t)\|,$$

$$\|W_1\Phi(x;t)\| = \left\|-\int_0^t [\lambda_2 + \lambda_3(t-\tau)]\,\Phi(x;\tau)d\tau\right\| \le \left\{|\lambda_2|\,T + |\lambda_3|\,\frac{T^2}{2}\right\}\|\Phi(x;t)\|, \tag{11}$$

$$\|W_2\Phi(x;t)\| \le g\frac{T^2}{2} C\|\Phi(x;t)\|.$$

Hence, we have

$$\|\overline{W}\Phi(x;t)\| \le \left|\frac{1}{\lambda_1}\right| G + \left|\frac{1}{\lambda_1}\right| D\|\Phi(x;t)\|,$$

$$D = T\left\{|\lambda_2| + |\lambda_3|\,\frac{T}{2} + g\frac{T}{2}C\right\}. \tag{12}$$

From inequality (12) we deduce that the operator $\overline{W}$ is bounded and maps the ball S_ρ into itself, where the radius of the sphere

$$\rho = \frac{G}{|\lambda_1| - D} \quad \Rightarrow \quad D = T\left\{|\lambda_2| + |\lambda_3|\frac{T}{2} + g\frac{T}{2}C\right\} < |\lambda_1| \tag{13}$$

Lemma 2 Under the assumptions (i)-(iii), the integral operator $\overline{W}$ is continuous. Moreover, it is a contraction mapping.

Proof. Assume $\Phi_1(x;t)$, $\Phi_2(x;t)$ are two different solutions of Equation (5), the integral operator (6) yields

$$\overline{W}(\Phi_1 - \Phi_2)(x;t) = \frac{1}{\lambda_1} W_1(\Phi_1 - \Phi_2)(x;t) + \frac{1}{\lambda_1} W_2(\Phi_1 - \Phi_2)(x;t)$$

$$W_1(\Phi_1 - \Phi_2)(x;t) = -\int_0^t [\lambda_2 + \lambda_3(t-\tau)](\Phi_1 - \Phi_2)(x,\tau)d\tau \tag{14}$$

$$W_2(\Phi_1 - \Phi_2)(x;t) = \int_0^t \int_{-1}^1 (t-\tau)g(\tau)k(|x-y|)(\Phi_1 - \Phi_2)(y;\tau)dyd\tau$$

Hence, we have

$$\left\|\overline{W}(\Phi_1 - \Phi_2)(x;t)\right\| \le \left|\frac{1}{\lambda_1}\right|\left\{|\lambda_2|T + |\lambda_3|\frac{T^2}{2} + g\frac{T^2}{2}C\right\}\|(\Phi_1 - \Phi_2)(x;t)\|$$

$$\le \left|\frac{1}{\lambda_1}\right| D\|(\Phi_1 - \Phi_2)(x;t)\| \tag{15}$$

$$D = T\left\{|\lambda_2| + |\lambda_3|\frac{T}{2} + g\frac{T}{2}C\right\}.$$

Hence, from Equation (15) the integral operator $\overline{W}$ is continuous. Moreover, under the condition $D < |\lambda_1|$, $\overline{W}$ is a contraction mapping.

In view of Lemma 1 and Lemma 2, we can state the following:

Theorem 1 The mixed integral Equation (5) has a unique solution under the condition

$$T\left\{|\lambda_2| + |\lambda_3|\frac{T}{2} + g\frac{T}{2}C\right\} < |\lambda_1|. \tag{16}$$

Proof. Proving this theory is based on proving two lemmas, the first lemma is proving that the integral operator $\overline{W}$ maps the space $L_2(-1,1)\times C[0,T]$ into itself, (see lemma1). And the second lemma proves that the integral operator $\overline{W}$ is continuous, (see lemma 2). Since the integral operator represents a contraction mapping, by applying Banach's fixed point theorem the solution is unique under the condition of theorem 1.

4. The convergence of the solution

To examine the behavior solution of Equation (5). We consider the following sequence

$$\{\Phi_1(x,t), \Phi_2(x,t), \ldots, \Phi_{n-1}(x,t), \Phi_n(x,t), \ldots\} \subset \{\Phi_i(x,t)\}_{i=0}^{\infty} \tag{17}$$

Hence, we have

$$L_n(x;t) = \frac{1}{\lambda_1}\int_0^t \int_{-1}^1 (t-\tau)g(\tau)k(|x-y|)L_{n-1}(y;\tau)dyd\tau - \frac{1}{\lambda_1}\int_0^t [\lambda_2 + \lambda_3(t-\tau)]L_{n-1}(x;\tau)d\tau \tag{18}$$

where

$$L_n(x;t) = \Phi_n(x;t) - \Phi_n(x;t), \quad \Phi_n(x,t) = \sum_{i=0}^{n} L_i(x,t), L_0(x,t) = H(x,t). \tag{19}$$

Applying the conditions (i)-(iii) and the Cauchy-Schwartz inequality, to obtain

$$\|L_n(x;t)\| \leq \frac{D}{|\lambda_1|}\|L_{n-1}(x;t)\|; \quad D = T\left\{|\lambda_2| + |\lambda_3|\frac{T}{2} + g\frac{T}{2}C\right\}. \tag{20}$$

By induction, we have

$$\|L_n(x;t)\| \leq \left(\frac{D}{|\lambda_1|}\right)^n G, \quad G = \frac{T^2}{2}f + \lambda_1\psi_1 T + \lambda_2\psi_2 T + \lambda_1\psi_1, \quad (f, \psi_1, \psi_2 - \text{ cons } \tan ts). \tag{21}$$

Taking the sum of both sides of inequality (21) and note that $\frac{D}{|\lambda_1|} < 1$, hence we have

$$\sum_{n=0}^{\infty}\|L_n(x;t)\| \leq \sum_{n=0}^{\infty}\left(\frac{D}{|\lambda_1|}\right)^n G \Leftrightarrow \Phi_{n\to\infty}(x;t) = \Phi(x;t) < \frac{|\lambda_1|G}{|\lambda_1| - D}. \tag{22}$$

The previous inequality leads us to decide that the solution $\Phi(x,t)$ is convergent.

5. The stability of the error

In this section, the researcher studies the stability of the error resulting from the analytical solution and the numerical solution.

Consider $\Phi_m(x,t)$ is the numerical solution of Equation (5)

$$\Phi_m(x;t) + \frac{1}{\lambda_1}\int_0^t [\lambda_2 + \lambda_3(t-\tau)]\Phi_m(x;\tau)d\tau - \frac{1}{\lambda_1}\int_0^t\int_{-1}^1 (t-\tau)g(\tau)k(|x-y|)\Phi_m(y;\tau)dyd\tau = \frac{1}{\lambda_1}H_m(x,t),$$

$$H_m(x,t)=\int_0^t (t-\tau)f_m(x;\,\tau)d\tau+\lambda_1 t\psi_1(x)+\lambda_2 t\psi_2(x)+\lambda_1\psi_1(x) \tag{23}$$

Hence, from (5) and (23) we get

$$Z_m(x;t)+\frac{1}{\lambda_1}\int_0^t[\lambda_2+\lambda_3(t-\tau)]Z_m(x;\,\tau)d\tau-\frac{1}{\lambda_1}\int_0^t\int_{-1}^1(t-\tau)g(\tau)k(|x-y|)Z_m(y;\,\tau)dyd\tau=\frac{1}{\lambda_1}U_m(x,t) \tag{24}$$

where $Z_m(x;t)$ is the error function, $Z_m(x,t)=\Phi(x,t)-\Phi_m(x,t)$ and the free function is given by

$$U_m(x,t)=H(x,t)-H_m(x,t)=\int_0^t(t-\tau)\left[f(x;\,\tau)-f_m(x;\,\tau)\right]d\tau \tag{25}$$

The error function takes the same form as the MIE. And it can be solved under the same assumption (i)-(iii). To discuss the existence of a unique solution to the error, we write (24) in the integral operator form.

$$\overline{B}Z_m(x;t)=\frac{1}{\lambda_1}U_m(x,t)-\frac{1}{\lambda_1}B_1Z_m(x;t)+\frac{1}{\lambda_1}B_2Z_m(x;t), \tag{26}$$

where

$$B_1Z_m(x;t)=\int_0^t[\lambda_2+\lambda_3(t-\tau)]Z_m(x;\,\tau)d\tau,\ B_2Z_m(x;t)=\int_0^t\int_{-1}^1(t-\tau)g(\tau)k(|x-y|)Z_m(y;\,\tau)dyd\tau \tag{27}$$

Lemma 3 The integral operator $\overline{B}$, under the assumptions (i)-(iii), maps the space $L_2(-1,\,1)\times C[0,\,T]$ into itself.
Proof. Following the same way as lemma 1, we have

$$\left\|\overline{B}Z_m(x;t)\right\|\le\left|\frac{1}{\lambda_1}\right|\|U(x;t)-U_m(x;t)\|+\left|\frac{1}{\lambda_1}\right|D\,\|Z_m(x;t)\|;\quad D=T\left\{|\lambda_2|+|\lambda_3|\,\frac{T}{2}+g\frac{T}{2}C\right\} \tag{28}$$

Hence, the operator $\overline{B}$ of inequality (28) is bounded and maps the ball S_σ into itself, where the radius of the sphere

$$\sigma=\frac{\|U(x;t)-U_m(x;t)\|}{|\lambda_1|-D}\Rightarrow D=T\left\{|\lambda_2|+|\lambda_3|\,\frac{T}{2}+g\frac{T}{2}C\right\}<|\lambda_1| \tag{29}$$

Lemma 4 The integral operator $\overline{B}$, under the condition (i)-(iii) is continuous. Moreover, it is a contraction mapping.
Proof. Let $Z_{m,\,1}(x;t),\,Z_{m,\,2}(x;t)$ be the two different error solutions of Equation (24), the integral operator (26) yields

$$\overline{B}\left(\Phi_1-\Phi_2\right)(x;t)=\frac{1}{\lambda_1}B_1\left(\Phi_1-\Phi_2\right)(x;t)+\frac{1}{\lambda_1}B_2\left(\Phi_1-\Phi_2\right)(x;t). \tag{30}$$

Following the same way as Lemma 2, we have

$$\|\bar{B}\left(Z_{m,1}-Z_{m,2}\right)(x;t)\| \leq \left|\frac{1}{\lambda_1}\right| D\,\|\left(Z_{m,1}-Z_{m,2}\right)(x;t)\|, \quad D = T\left\{|\lambda_2|+|\lambda_3|\,\frac{T}{2}+g\frac{T}{2}C\right\} \tag{31}$$

The above inequality proves the continuity of the error function. Moreover, under the condition $D<|\lambda_1|$ the integral operator $\overline{B}$ is a contraction mapping. Hence, we can consider the following:

Theorem 2 The error function of Equation (24) has a unique solution under the condition

$$T\left\{|\lambda_2|+|\lambda_3|\,\frac{T}{2}+g\frac{T}{2}C\right\}<|\lambda_1|. \tag{32}$$

The proof of the theory is obtained directly from Lemma 3 and Lemma 4.

Theorem 3 The error $Z_m(x;t)$, $m\to\infty$, is vanishing.

Proof. Since the radius of the sphere of convergence is $\sigma=\frac{\|U(x;t)-U_m(x;t)\|}{|\lambda_1|-D}$, then let $m\to 0$, we have $\sigma\to 0$ this leads directly, from Equation (28) to say that $Z_{m\to\infty}(x;t)=0$.

6. Technique of separation

The separation of variables method in the new technique is used, in this section to obtain an FIE with discontinuous kernel. The coefficients of FIE are variable in time. For this assume the solution of Equation (5), in the form:

$$\Phi(x,t)=\sum_{n=0}^{\infty}\psi_n(x)t^n,\ f(x,t)=\sum_{n=0}^{\infty}f_n(x)t^n;\quad t\in[0,T];T<1,\quad n=1,2,\ldots, \tag{33}$$

The series in Equation (33) is absolutely convergent and when $n\to\infty$ the two functions $\Phi(x,t)=\frac{\psi_\infty(x)}{1-t}$, $f(x,t)=\frac{f_\infty(x)}{1-t}$, $0\leq t<1$. Therefore, we assume n is a finite number.

After using Equation (33) in Equation (5), we have

$$\psi_n(x)-\frac{B(t,n)}{A\left(t,n,\lambda_i\right)}\int_{-1}^{1}k\left(|x-y|\,\middle|\,\psi_n(y)dy=\frac{H_n(x)}{A\left(t,n,\lambda_i\right)}t^n\right.,\ (i=1,2,3,n=0,1,2,\ldots,), \tag{34}$$

where

$$A\left(t,n,\lambda_i\right)=t^n\left[\lambda_1+\frac{t\lambda_2}{(n+1)}+\frac{t^2\lambda_3}{(n+1)(n+2)}\right],\ B(t,n)=\int_0^t(t-\tau)g(\tau)\tau^n d\tau$$
$$H_n(x)t^n=\frac{t^{n+2}}{(n+1)(n+2)}f_n(x)+t\left(\lambda_1\psi_1(x)+\lambda_2\psi_2(x)\right)+\lambda_1\psi_1(x) \tag{35}$$

The formula (34) represents a system of FIEs with a discontinuous kernel and its coefficients are functions of the constants λ_1, λ_2, λ_3 beside the time t and its pour n. In this case, the condition for a unique solution of Equation (34) is $\|k|x-y|\|\left|\frac{B(t,n)}{A(t,n,\lambda_i)}\right|<1$.

7. Numerical method (Toeplitz matrix method), see[5, 22, 27]

The TMM is one of the most powerful and best numerical methods for solving anomalous integral equations. First, it is solved by assuming a general anomalous kernel, and then the other anomalous cases studied are considered as special cases derived from the original kernel. Second, this method transforms anomalous integrals into simple numerical integrals that can be calculated. Third, the convergence of the error is much better than other methods, especially in anomalous integral equations. Therefore, we will assume a general form of the FIE with a general anomalous kernel as follows: Consider the FIE of the second kind:

$$\varphi(x)-\lambda(t)\int_{-1}^{1}k(|x-y|)\varphi(y)dy=f(x) \tag{36}$$

Write the integral term in the form

$$\int_{-1}^{1}k(|x-y|)\varphi(y)dy=\sum_{n=-N}^{N-1}\int_{nh}^{nh+h}k(|x-y|)\varphi(y)dy \tag{37}$$

Following the same way of [5, 22, 27], we have

$$\varphi(x)-\lambda(t)\sum_{n-N}^{N-1}D_n(x)\varphi(nh)=f(x) \tag{38}$$

where

$$D_n(x)=\begin{cases}A_{-N}(x), & n=-N\\ A_n(x)+B_{n-1}(x), & -N<n<N\\ B_{N-1}(x), & n=N\end{cases} \tag{39}$$

If we put $x=mh$, in Equation (39) and then adapt the formula (39) to take the form

$$\varphi(mh)-\lambda(t)a_{n,m}\varphi(nh)=f(mh),\quad -N\le n,m\le N. \tag{40}$$

The function ϕ is a vector of $2N+1$ elements. But $a_{n,m}$ is a matrix whose elements are given by

$$a_{n,m} = a'_{n,m} + g_{n,m}$$
$$a'_{n,m} = A_n(mh) + B_{n-1}(mh), \quad -N \le n \le N \tag{41}$$

The matrix $a'_{n,m}$, in Equation (41), is the Toeplitz matrix of order $2N+1$, where $-N \le m, n \le N$ and the elements of the second matrix $g_{n,m}$ are zeros except the elements of the first and last rows. We can evaluate the values of the first row by substituting in $B_{n-1}(mh)$, $n = -N$, $m = -N+i$, $0 \le i \le 2n$ and the values of the last row by substituting in $A_n(mh)$, by $n = N$, $m = -N+i$.

The solution of the formula (40) takes the form

$$\varphi(mh) = [I - \lambda(t)a_{n,m}]^{-1} f(mh), |I - \lambda(t)a_{n,m}| \neq 0 \quad \forall t \in [0, T], T < 1, \tag{42}$$

where, in Equation (42), I is the identity matrix of order $2N+1$.

Lemma 5 (see Abdou et al. [27]). The TMM is said to be convergent of order r in $[-a, a]$. If for N sufficiently large, there exists a constant $D > 0$ independent of N such that

$$\|\phi(x) - \phi_N(x)\| \le DN^{-r} \tag{43}$$

Lemma 6 (see Abdou et al. [23]). The error term R is determined from the following formula

$$R = \left| \int_{nh}^{nh+h} y^2 k(|x-y|)dy - A_n(x)(nh)^2 - B_n(x)(nh+h)^2 \right| = O\left(h^3\right) \tag{44}$$

8. Numerical results

In application tables and numerical examples, the following abbreviations will be used:

Exact solution	$\Phi_E(x, t)$	E.S
Approximate solution for Carleman (logarithmic) kernel	$\Phi_{N.Car.}(x, t)\ (\Phi_{N.\log.}(x, t))$	Carl. (Log.) Approx
The numerical error resulting from the calculation of the Carleman (logarithmic) kernel	$R_{\text{car.}} = \|\Phi_{E.}(x, t) - \Phi_{N.Car.}(x, t)\|$ $R_{\log.} = \|\Phi_{E.}(x, t) - \Phi_{N.\log.}(x, t)\|$	Carl. (Log.) Error

Application 1: Consider in Eequation (5) the following data $\lambda_1 = 1$, $\lambda_2 = 0.02$, $\lambda_3 = 0.04$, $g(t) = t^2$ and the exact solution is $\Phi(x, t) = x^2t^2$.

Hence, the free term takes the form

$$H(x) = \left\{1 + \frac{t}{150} + \frac{t^2}{300}\right\} x^2 + \frac{t^2}{12} \int_{-1}^{1} k|(x-y)|y^2 dy \tag{45}$$

For the logarithmic kernel and Carleman kernel under the above data, we have

Table 1. The approximate solution and the error compactional for the Logarithmic kernel and Carleman kernel at $N = 41$, $T = 0.6$

x	E.S	Carl. Approx. sol.	Carl. Error	Log. Approx. sol.	Log. Error
-1	0.36	0.3719509342	1.19509E-02	0.361294835	1.29483E-03
-0.8	0.2304	0.234694616	4.29462E-03	0.230026695	3.73305E-04
-0.6	0.1296	0.130779427	1.17943E-03	0.129074204	5.25796E-04
-0.4	0.0576	0.057703421	1.03421E-04	5.71628E-02	4.37231E-04
-0.2	0.0144	0.014328343	7.16567E-05	1.41649E-02	2.35051E-04
0	0.00000E+00	0.00000E+00	0.00000E+00	0.00000E+00	0.00000E+00
0.2	0.0144	0.01450683	1.06830E-04	1.46396E-02	2.39574E-04
0.4	0.0576	0.058064966	4.64966E-04	5.81094E-02	5.09398E-04
0.6	0.1296	0.131347144	1.74714E-03	0.130489404	8.89404E-04
0.8	0.2304	0.235583977	5.18398E-03	0.231914934	1.51493E-03
1	0.36	0.3727919109	1.27919E-02	0.362581676	2.58168E-03

The result of Table 1 is obtained when the discontinuous kernel, in Equation (5) takes the form of Logarithmic kernel and Carleman function with exact solution $\Phi(x, t) = x^2t^2$ and consider the following data: $\lambda_1 = 1$, $\lambda_2 = 0.02$, $\lambda_3 = 0.04$, $g(t) = t^2$, $\mathrm{N} = 41$, $\mathrm{T} = 0.6$.

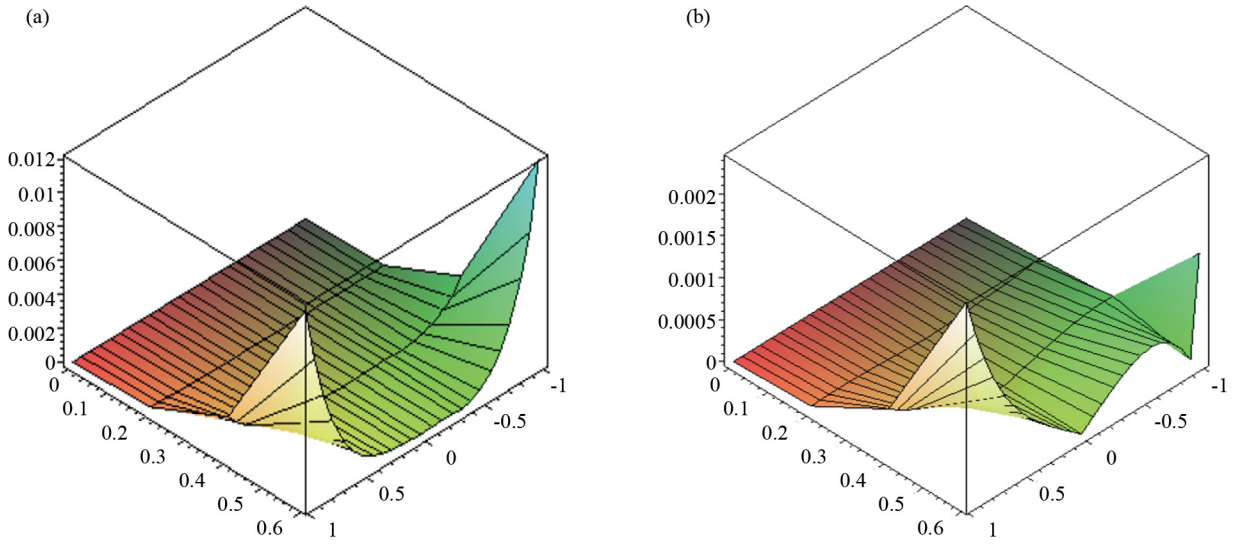

Figure 1. (a) Carleman Error; (b) Logarithmic error

Figure 1 is obtained when the discontinuous kernel, in Equation (5) takes the form of Logarithmic kernel and Carleman function with exact solution $\Phi(x, t) = x^2t^2$ and consider the following data: $\lambda_1 = 1$, $\lambda_2 = 0.02$, $\lambda_3 = 0.04$, $g(t) = t^2$, $\mathrm{N} = 41$, $\mathrm{T} = 0.6$.

Application 2: Consider in Equation (5) the following data $\lambda_1 = 1$, $\lambda_2 = 0.03$, $\lambda_3 = 0.012$, $g(t) = t^2$, $N = 41$, $T = 0.02$ and the exact solution is $\Phi(x, t) = x^2t^2$. Hence, the free term takes the form $H(x) = \left\{1 + \frac{t}{100} + \frac{t^2}{10}\right\}x^2 + \frac{t^2}{12}\int_{-1}^{1} k|(x-y)|y^2dy$.

Table 2. The approximate solution and the error compactional for the Logarithmic kernel and Carleman kernel at $N = 41$, $T = 0.02$

x	E.S	Carl. Approx. sol.	Carl. Error	Log. Approx. sol.	Log. Error
-1	4.00E-04	3.99185E-04	8.15003E-07	3.98278E-04	1.72165E-06
-0.8	2.56E-04	2.54986E-04	1.01366E-06	2.54210E-04	1.79010E-06
-0.6	1.44E-04	1.43373E-04	6.26946E-07	1.42935E-04	1.06500E-06
-0.4	6.40E-05	6.36282E-05	3.71772E-07	6.33866E-05	6.13373E-07
-0.2	1.60E-05	1.58227E-05	1.77329E-07	1.57112E-05	2.88757E-07
0	0.0E+00	0.00000E+00	0.00000E+00	0.00000E+00	0.00000E+00
0.2	1.60E-05	1.61749E-05	1.74881E-07	1.62836E-05	2.83614E-07
0.4	6.40E-05	6.43326E-05	3.32580E-07	6.45311E-05	5.31059E-07
0.6	1.44E-04	1.44429E-04	4.28519E-07	1.44648E-04	6.48295E-07
0.8	2.56E-04	2.56386E-04	3.86450E-07	2.56473E-04	4.73102E-07
1	4.00E-04	4.00094E-04	9.37946E-08	3.99762E-04	2.38382E-07

In Table 2, we consider the following data: $\lambda_1 = 1$, $\lambda_2 = 0.03$, $\lambda_3 = 0.012$, $g(t) = t^2$ $N = 41$, $T = 0.02$, and the exact solution $\Phi(x, t) = x^2t^2$. The kernel takes the form of a Logarithmic kernel and Carleman function.

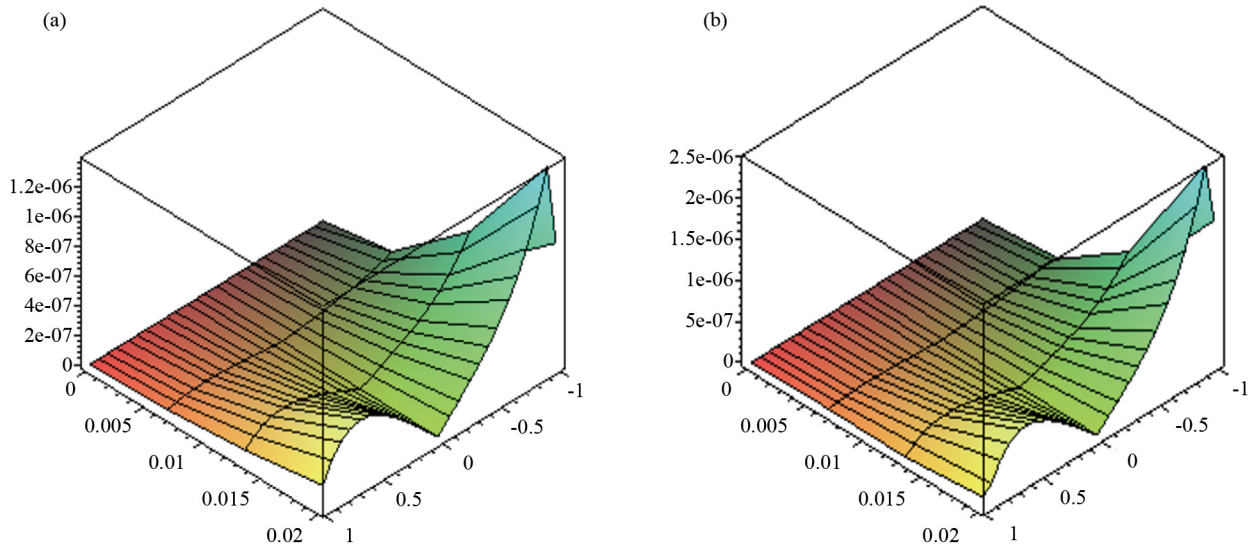

Figure 2. (a) Carleman error; (b) Logarithmic error

In Figure 2, we consider the following data: $\lambda_1 = 1$, $\lambda_2 = 0.03$, $\lambda_3 = 0.012$, $g(t) = t^2$ N = 40, T = 0.02, and the exact solution $\Phi(x, t) = x^2t^2$. The kernel takes the form of a Logarithmic kernel and the Carleman function.

Application 3: Consider the same data as application 2 at $T = 0.004$.

Table 3. The approximate solution and the corresponding error for the Carleman kernel and logarithmic kernel

x	E.S	Carl. Approx. sol.	Carl. Error	Log. Approx. sol.	Log. Error
-1	1.600E-05	1.59674E-05	3.26242E-08	1.59311E-05	6.88737E-08
-0.8	1.024E-05	1.01994E-05	4.05566E-08	1.01684E-05	7.16074E-08
-0.6	5.760E-06	5.73492E-06	2.50813E-08	5.7174E-06	4.2601E-08
-0.4	2.560E-06	2.54513E-06	1.48718E-08	2.53546E-06	2.45352E-08
-0.2	6.400E-07	6.32907E-07	7.09334E-09	6.2845E-07	1.15504E-08
0	0.000E+00	0.00000E+00	0.00000E+00	0.00000E+00	0.00000E+00
0.2	6.400E-07	6.46995E-07	6.99532E-09	6.51345E-07	1.13446E-08
0.4	2.560E-06	2.57330E-06	1.33028E-08	2.58124E-06	2.12423E-08
0.6	5.760E-06	5.77714E-06	1.7138E-08	5.78593E-06	2.5931E-08
0.8	1.024E-05	1.02554E-05	1.54485E-08	1.02589E-05	1.89211E-08
1	1.600E-05	1.60037E-05	3.72765E-09	1.59905E-05	9.54287E-09

In Table 3, we consider the following data $\lambda_1 = 1$, $\lambda_2 = 0.03$, $\lambda_3 = 0.012$, $g(t) = t^2$ N = 41, T = 0.004, and the exact solution $\Phi(x, t) = x^2t^2$. The kernel takes the form of a Logarithmic kernel and the Carleman function.

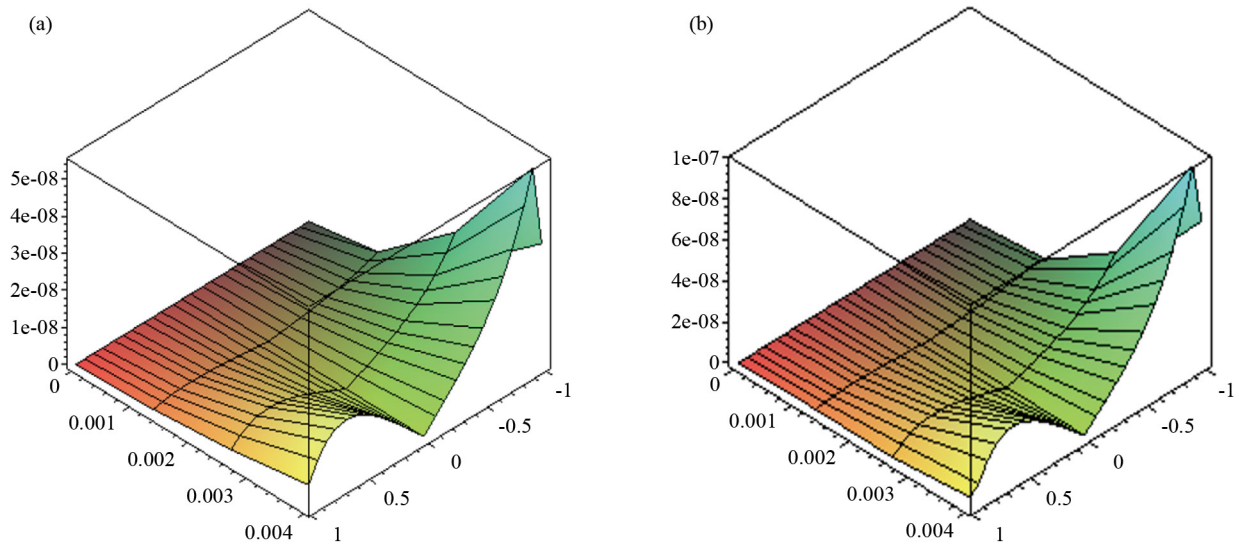

Figure 3. (a) Carleman Error; (b) Logarithmic error

In Figure 3, we consider $\lambda_1 = 1$, $\lambda_2 = 0.03$, $\lambda_3 = 0.012$, $g(t) = t^2$ N = 40, T = 0.004, and the exact solution $\Phi(x, t) = x^2t^2$. The kernel takes the form of a Logarithmic kernel and Carleman function.

9. Discussion

It is noted from the numerical results obtained, which we linked to time, with the other parameters being constant, the following: The shorter the time, the smaller the cumulative error of the solution, and vice versa. When the time increases, the error increases as a result of the accumulation of errors from previous times. We prove this with what we have reached.

(i) At $T = 0.6$: The error of the logarithmic kernel is less than the error of the Carleman kernel. The minimum value of the error at $x = -1$ and its value is 1.29483E-03.

(ii) At $T = 0.02$: The minimum error at $x = -1$ for the logarithmic kernel and its value is 1.72165E-06. Also, the error of the logarithmic kernel is less than the error of the Carleman kernel.

(iii) At $T = 0.004$: The minimum error is for the logarithmic kernel with value 1.13446E-08 at $x = 0.2$. In addition, the error of the logarithmic kernel is less than the error of the Carleman kernel.

It is noted that the stability of other parameters was considered.

10. Conclusion

From the above numerical results, we can establish the following:

(1) Analytical or semi-analytical methods cannot be used to solve this type of equation.

(2) The Toeplitz matrix method is one of the most powerful numerical methods for solving anomalous integral equations, as its use transforms the anomalous integral part into ordinary integrals that can be calculated.

(3) The method used in the paper put the anomalous nucleus in a general state, and then it was possible to derive many special nuclei from it, which was not possible using classical numerical methods.

(4) The time-delayed phase integro equation is a form of the integral partial differential equation.

(5) The time-dependent integro partial differential equation, after integration under initial conditions, is transformed into a mixed integral equation of the Volterra-Fredholm type.

(6) Using the separation of variables technique, we obtain the Fredholm integral equation with time-varying coefficients and position constants.

(7) One of the most famous and powerful numerical methods is the compact matrix method, as it deals with an anomalous kernel in general. Through this kernel, many other anomalous kernels can be derived as a special case of this kernel. In addition, the anomalous integrals are transformed into ordinary integrals that are easy to calculate.

Future work: we will try to discuss the solution of the nonlinear integro partial differential equation

$$\lambda_1 \frac{\partial^2}{\partial t^2}\Phi(x;t) + \lambda_2 \frac{\partial}{\partial t}\Phi(x;t) + \lambda_3 \Phi(x;t) - g(t)\int_{-1}^{1} k(|x-y|)\Phi^p(y;t)dy = f(x;t)$$

$$\left\{ \frac{\partial}{\partial t}\Phi(x;0) = \Psi_1(x), \Phi(x,0) = \Psi_2(x), 1 \le p \le N \right\} \tag{46}$$

Ethical approval

This manuscript does not contain any studies with human participants or animals performed by any of the authors.

Data availability

The data may be available from authors on reasonable request.

Authorship contributions

All authors contributed to the study's conception and design. The authors performed material preparation, data collection, and analysis. The author read and approved the final paper.

Conflict of interest

The author declares no competing financial interest.

References

[1] Abdou MA. Fredholm-Volterra integral equation of the first kind and contact problem. *Journal of Applied Mathematics and Computing*. 2002; 125: 177-193.

[2] Abdou MA. On the solution of linear and nonlinear integral equation. *Applied Mathematics and Computation*. 2004; 151: 132-145.

[3] Alahmadi J, Abdou MA, Abdel-Aty MA. Analytical and numerical treatment of a nonlinear Fredholm integral equation in two dimensions. *Journal of Applied Mathematics and Computing*. 2024; 71: 1-27. Available from: https://doi.org/10.1007/s12190-024-02264-4.

[4] Matoog RT, Mahdy AMS, Abdou MA, Mohamed DSA. Computational method for solving nonlinear fractional integral equations. *Fractal and Fractional*. 2024; 8: 663. Available from: https://doi.org/10.3390/fractalfract8110663.

[5] Raad SA, Abdou MA. An algorithm for the solution of integro-fractional differential equations with a generalized symmetric, singular kernel. *Fractal and Fractional*. 2024; 8: 644. Available from: https://doi.org/10.3390/fractalfract8110644.

[6] Rostami Y, Maleknejad K. Approximate solution to solve singular variable-order fractional Volterra-Fredholm integral partial differential equations type defined using hybrid functions. *International Journal of Computer Mathematics*. 2024; 101(6): 668-693. Available from: https://doi.org/10.1080/00207160.2024.2371604.

[7] Abdou MA, Allamakee MN, Soliman AA, Mosa GA. The behavior of the maximum and minimum error for Fredholm-Volterra integral equations in two-dimensional space. *Journal of Interdisciplinary Mathematics*. 2021; 24(4): 1-22.

[8] Basseem M, Alalyani A. On the solution of quadratic nonlinear integral equation with different singular kernels. *Mathematical Problems in Engineering*. 2020; 2020(1): 7856207.

[9] Matoog RT. Existence of at least one solution of singular Volterra-Hammerstein integral equation and its numerical solution. *African Journal of Mathematical and Computer Science Research*. 2016; 9(3): 15-23.

[10] Matoog RT. Modified Taylor's method and nonlinear mixed integral equation. *Universal Journal of Integral Equations*. 2016; 4: 21-29.

[11] Micula S. On some iterative numerical methods for a Volterra functional integral equation of the second kind. *Journal of Fixed Point Theory and Applications*. 2017; 19(3): 1815-1824.

[12] Mirzaee F, Hoseini SF. Application of Fibonacci collocation method for solving Volterra-Fredholm integral equations. *Applied Mathematics and Computation*. 2016; 273: 637-644.

[13] Nasr ME, Abdel-Aty MA. Analytical discussion for the mixed integral equations. *Journal of Fixed Point Theory and Applications*. 2018; 20(3): 115.

[14] Matoog RT. Treatments of probability potential function for a nuclear integral equation. *Journal of Physics and Mathematics*. 2017; 8(2): 226.

[15] Basseem M. Degenerate method in mixed nonlinear three dimensions integral equation. *Alexandria Engineering Journal*. 2019; 58: 387-392.

[16] Abdou MA, Soliman AA, Abdel-Aty MA. Analytical results for quadratic integral equations with phase lag term. *Journal of Applied Analysis and Computation*. 2020; 20(4): 1588-1598.

[17] Rostami Y, Maleknejad K. A novel approach to solving system of integral partial differential equations based on hybrid modified block-pulse functions. *Mathematical Methods in the Applied Sciences*. 2024; 47(7): 5798-5818. Available from: https://doi.org/10.1002/mma.9891.

[18] Rostami Y, Maleknejad K. Comparison of two hybrid functions for numerical solution of nonlinear mixed partial integro-differential equations. *Iranian Journal of Science and Technology, Transactions A: Science*. 2022; 46(2): 645-658. Available from: https://doi.org/10.1007/s40995-022-01277-7.

[19] Xie J. Numerical computation of fractional partial differential equations with variable coefficients utilizing the modified fractional Legendre wavelets and error analysis. *Mathematical Methods in the Applied Sciences*. 2021; 44(8): 7150-7164.

[20] Xie J, Wang T, Ren Z, Zhang J, Quan L. Haar wavelet method for approximating the solution of a coupled system of fractional-order integral-differential equations. *Mathematics and Computers in Simulation*. 2019; 163: 80-89.

[21] Xie J, Yao Z, Gui H, Zhao F, Li D. A two-dimensional Chebyshev wavelets approach for solving the Fokker-Planck equations of time and space fractional derivatives type with variable coefficients. *Applied Mathematics and Computation*. 2018; 332: 197-208.

[22] Jan AR. On a model for solving mixed fractional integrodifferential equation. *Contemporary Mathematics*. 2024; 5(4): 6067-6081. Available from: http://ojs.wiserpub.com/index.php/CM/.

[23] Sayed SM, Mohamed AS, Abo-Eldahab EM, Youssri YH. Spectral framework using modified shifted Chebyshev polynomials of the third-kind for numerical solutions of one- and two-dimensional hyperbolic telegraph equations. *Boundary Value Problems*. 2025; 2025(1): 7.

[24] Ezz-Eldien SS, Alalyani A. Legendre spectral collocation method for one- and two-dimensional nonlinear pantograph Volterra-Fredholm integro-differential equations. *International Journal of Modern Physics C*. 2025; 2550061. Available from: https://doi.org/10.1142/S0129183125500615.

[25] Yassin NM, Atta AG, Aly EH. Numerical solutions for nonlinear ordinary and fractional Newell-Whitehead-Segel equation using shifted Schröder polynomials. *Boundary Value Problems*. 2025; 2025(1): 57. Available from: https://doi.org/10.1186/s13661-025-02041-7.

[26] Abd-Elhameed WM, Youssri YH, Atta AG. Tau algorithm for fractional delay differential equations utilizing seventh-kind Chebyshev polynomials. *Journal of Mathematical Modeling*. 2024; 12(2): 277-299. Available from: https://doi.org/10.22124/jmm.2024.25844.2295.

[27] Abdou MA, El-Borai MM, El-Kojok MM. Toeplitz matrix method and nonlinear integral equation of Hammerstein type. *Journal of Computational and Applied Mathematics*. 2009; 223: 765-776.